

Available at www.sciencedirect.com

ScienceDirect

journal homepage: www.elsevier.com/locate/jff

Multi-faceted integrated omics analysis revealed parsley (*Petroselinum crispum*) as a novel dietary intervention in dextran sodium sulphate induced colitic mice

Huijuan Jia^{a,1}, Wanping Aw^{a,b,c,1}, Manaka Hanate^d, Shoko Takahashi^d, Kenji Saito^a, Hiroshi Tanaka^b, Masaru Tomita^c, Hisanori Kato^{a,d,*}

^a Corporate Sponsored Research Program “Food for Life”, Organization for Interdisciplinary Research Projects, The University of Tokyo, Japan

^b Graduate School of Biomedical Science, Tokyo Medical and Dental University, Japan

^c Institute for Advanced Biosciences, Keio University, Japan

^d Department of Applied Biological Chemistry, Graduate School of Agricultural and Life Sciences, The University of Tokyo, Japan

ARTICLE INFO

Article history:

Received 14 August 2014

Received in revised form 26

September 2014

Accepted 29 September 2014

Available online 12 November 2014

Keywords:

Inflammatory bowel disease

Metabolome

Parsley supplementation

Proteome

Transcriptome

ABSTRACT

Here we describe our unprecedented approach in proposing parsley as a nutraceutical intervention in inflammatory bowel disease (IBD) via multi-omics evaluation using dextran sodium sulphate (DSS)-induced colitis. Seven-week-old male C57BL/6J mice were fed either 2% parsley or basal diet and drank normal-drinking-water for 1 week after which colitis was induced by administering 1.5% (w/v) DSS-drinking-water for 9 days. Parsley supplementation significantly improved colon shortening and increased disease activity index. Colonic transcriptome revealed down-regulation of inflammatory cytokines, hepatic transcriptome and metabolome revealed up-regulation of fatty-acid synthesis genes, thereby improving body weight loss. Down-regulated cancer markers were observed in the hepatic transcriptome and proteome. Plasma metabolite analysis indicated shifts in the citric and urea cycle, implicating improved impaired glycolysis and oxidative stress. Parsley's role in preventing against IBD was highlighted by this pioneering multi-integrated-omics which is expected to be useful and informative, and shape the future of nutraceutical and functional food research.

© 2014 The Authors. Published by Elsevier Ltd. This is an open access article under the CC BY-NC-ND license (<http://creativecommons.org/licenses/by-nc-nd/3.0/>).

* Corresponding author. Organization for Interdisciplinary Research Projects, The University of Tokyo, 1-1-1, Yayoi, Bunkyo-ku, Tokyo 113-8657, Japan. Tel.: +81 3 5841 1607; fax: +81 3 5841 1607.

E-mail address: akatoq@mail.ecc.u-tokyo.ac.jp (H. Kato).

¹ These authors contributed equally to this work.

Abbreviations: AA, amino acid; Ala, alanine; Asn, asparagine; Asp, aspartic acid; Arg1, arginase 1; Ccl, chemokine (C-C motif) ligand; Cebp/d, CCAAT/enhancer binding protein (C/EBP), delta; Cd163, cluster of differentiation 163; Cxcl, chemokine (C-X-C motif) ligand; DAI, disease activity index; DSS, dextran sodium sulphate; Elovl6, ELOVL family member 6, elongation of long chain fatty acids; Fas, fatty acid synthase; Got1, glutamic-oxaloacetic transaminase 1; H&E, hematoxylin and eosin; Hp, haptoglobin; IBD, inflammatory bowel disease; Ile, isoleucine; iTRAQ, isobaric tag for relative and absolute quantitation; Jun, c-Jun; Mat2a, methionine adenosyltransferase II, alpha; Mdh1, malate dehydrogenase 1; Me1, NADP-dependent malic enzyme; Met, methionine; MMP, metalloproteinase; Oat, argininosuccinate lyase; PAR, parsley; PCA, principal component analysis; Pla2g, phospholipase A2; Ptg2, prostaglandin-endoperoxide synthase 2; Rplp1, 60S acidic ribosomal protein P1; S100A8, S100 calcium binding protein A8; SAA1, serum amyloid A1; SCD1, stearoyl-CoA desaturase-1; Ser, serine; Spp1, secreted phosphoprotein 1; Thr, threonine; Timp1, tissue inhibitor of metalloproteinase 1; TNF, tumor necrosis factor; Val, valine; Vcam1, vascular cell adhesion protein 1

<http://dx.doi.org/10.1016/j.jff.2014.09.018>

1756-4646/© 2014 The Authors. Published by Elsevier Ltd. This is an open access article under the CC BY-NC-ND license (<http://creativecommons.org/licenses/by-nc-nd/3.0/>).

1. Introduction

Inflammatory bowel disease (IBD) includes Crohn's disease and ulcerative colitis which are chronic, remittent or progressive immunologically mediated disorders that affect the entire gastrointestinal tract or the colonic tract, respectively (Khor, Gardet, & Xavier, 2011). The precise etiology of IBD is unknown, but it is increasingly clear that IBD is a complex multifactorial disease involving genetic predisposition, intestinal microbiota, environmental factors (including diet) and the immune system (Baumgart & Carding, 2007). Many IBD patients have been reported to become dependent and cannot be withdrawn from treatment without a return of symptoms. Therefore, there are needs for better therapeutic agents that can effectively induce remission and alter the natural course of the disease with minimum or no side effects.

Parsley (*Petroselinum crispum*, PAR), a biennial plant native to Europe and Western Asia, is used as a culinary herb, condiment and garnish because of its special aroma; it is used on meat, fish, and vegetables, and in marinades, sauces and stuffing (Simon & Quinn, 1988). PAR contains abundant antioxidants (luteolin and apigenin) (Justesen, Knuthsen, & Leth, 1998), folic acid, and vitamins K, C, and A. Traditionally, PAR leaves have been used in the treatment of inflammatory conditions, mastitis, hematomata, constipation, flatulence, jaundice, colic, edema, rheumatism, as well as diseases of the prostate and liver (Simon & Quinn, 1988).

In the present study, using a nutrigenomics approach—the goal of which is to understand nutrients as dietary signals that influence gene and protein expressions and subsequently, metabolite production—we sought to identify the dietary signature of PAR interactions and to uncover potential novel mechanisms in a dextran sodium sulphate (DSS)-induced colitic murine model by conducting global transcriptome, proteome and metabolome analyses using colon tissue, liver tissue and plasma.

2. Materials and methods

2.1. Animals and dietary treatment

Seven-week-old male C57BL6/J mice obtained from Charles River Japan (Tokyo, Japan) were housed individually in animal cages in a room with controlled temperature ($23 \pm 2^\circ\text{C}$), humidity ($50 \pm 10\%$), and lighting (lights on from 08:00 to 20:00). After 3 days of acclimatization, the mice were divided into three groups ($n = 7$) with equal mean body weights: (1) mice given a AIN-93G basal diet and normal drinking water for the course of the entire experiment (CON group), (2) mice given the AIN-93G basal diet and normal drinking water for 1 week, after which colitis was induced by administering 1.5% (w/v) DSS (DSS molecular weight, 40 KDa; MP Biomedicals, Irvine, CA, USA)-containing drinking water (DSS group); and (3) mice given a 2% freeze-dried PAR powder (House Foods Group Inc., Tokyo, Japan)-supplemented AIN-93G basal diet and normal drinking water for 1 week, then 1.5% DSS-containing drinking water (DSSPAR group) for 9 days. The 2% PAR diet was adjusted with cornstarch to maintain caloric balance as shown in Table 1. We chose

Table 1 – Composition of diet.

Formula	AIN-93G basal diet	2% Parsley
Ingredients (%)		
Ground parsley powder	–	2
Casein	20	20
Cornstarch	39.75	37.75
Detrized cornstarch	13.2	13.2
Sucrose	10.25	10.25
Soybean oil	7	7
Fiber	5	5
Mineral mix	3.5	3.5
Vitamin mix	1	1
L-Cystine	0.3	0.3
Energy (kJ)	1559.5	1557.1

a 2% PAR supplemented diet in this study based on previous results of a dose-dependent study. Animal care and treatment were conducted in accordance with the institutional guidelines of the University of Tokyo (Approval Number: P13-739).

2.2. Evaluation of the disease activity index

The body weight, stool consistency and fecal blood of the mice were recorded daily after the induction of colitis. The disease activity index (DAI) was calculated by combining these three scores and then dividing the score by 3. Each score was determined as follows: change in body weight (0: <1%; 1: 1–5%; 2: 5–10%; 3: 10–15%; 4: >15%), fecal blood (0: no fecal blood observed, 2: ++, 4: ++++) and stool consistency (0: normal, 2: soft, 4: diarrhea) (Islam et al., 2009; McHenga, Wang, Li, Shan, & Lu, 2008).

2.3. Blood collection and tissue harvesting

At the time of sacrifice, the mice were deeply anesthetized with sodium pentobarbital followed by bleeding from the carotid artery. Plasma was obtained by centrifuging blood at $1000 \times g$ for 15 min at 4°C . Colon length was measured as the distance between the ileo-cecal junction and the proximal rectum. Excised colon tissue, liver tissue and mesenteric adipose tissues were snap-frozen in liquid nitrogen and stored at -80°C until further analysis.

2.4. Biochemical assays

Colonic myeloperoxidase activity (MPO) was measured colorimetrically (BioVision Inc., CA, USA) and concentrations of plasma IL6, plasma serum amyloid A1 (SAA1) and plasma matrix metalloproteinase-3 (MMP3) were measured by using the ELISA (Thermo Scientific, Rockford, IL, USA; Cusabio Biotech Co., Ltd., Hubei, China; and R&D Systems Inc., Minneapolis, MN, USA, respectively), according to manufacturer's instructions.

2.5. Colon histology

Part of the colon was embedded in Optimal Cutting Temperature compound (Sakura Finetek, Torrance, CA, USA), and then

snap-frozen in liquid nitrogen. The tissues were sectioned at 5- μ m-thick and stained with hematoxylin and eosin (H&E), and then scanned by light microscopy (200 \times , Olympus BX51 microscope, Olympus Optical, Tokyo, Japan).

2.6. Total RNA extraction and quality assessment

Total RNA was extracted from the frozen liver and colon samples using the total RNA Isolation Kit, NucleoSpin® RNA II (Macherey-Nagel, Düren, Germany) and Trizol (Jia et al., 2013; Jia, Takahashi, Saito, & Kato, 2013), respectively, according to the manufacturers' instructions. The RNA concentration and purity were determined using a NanoDrop ND-1000 spectrophotometer (NanoDrop Technologies, Wilmington, DE, USA). RNA purity was assessed by using the Agilent 2100 Bioanalyzer (Agilent Technologies, Santa Clara, CA, USA). RNA integrity numbers were higher than 8.0.

2.7. Transcriptome analysis

2.7.1. DNA microarray preparation

Total hepatic and colonic RNA from each respective group were pooled ($n = 7$). The microarray analysis was carried out as described previously in Jia et al. (2013). Mouse Genome 430 2.0 Array GeneChips (Affymetrix, Santa Clara, CA, USA) containing over 30,000 gene probe sets were used for genome-wide expression profiling.

2.7.2. Mapping and ingenuity pathway functional analysis

The scanned images were analyzed with Microarray Suite version 5.0 (Affymetrix) for comparing gene expression ratios between the CON vs. DSS or DSS vs. DSSPAR groups. Genes showing expression ratios between treatments of more than 1.5-fold were considered differentially expressed. These genes were then selected and mapped using the Pathway Explorer function of Ingenuity Pathway Analysis (IPA, <http://www.ingenuity.com/>, date accessed: May 2013).

2.8. Reverse transcription polymerase chain reaction

RT-PCR was carried out as reported in Jia et al. (2013). Primer sequences are as shown in Supplementary Table S1. The relative amounts of mRNA were normalized to 60S acidic ribosomal protein P1 (Rplp1) expression levels in each sample, and the data are presented as the fold change of normalized mRNA amounts of each sample to those of the DSS group.

2.9. Protein preparation, iTRAQ labeling and NanoLC-MS/MS analysis for proteome analysis

Total protein was extracted by using lysis buffer and separated by centrifugation at 12,000 $\times g$ for 30 min at 4 °C. Protein concentrations were determined using the Bradford assay. Pooled protein (100 μ g) were treated for cysteine blocking and digested, then labeled with the isobaric tag for relative and absolute quantitation (iTRAQ) tags as follows: CON, 114 tag; DSS, 115 tag; DSSPAR, 116 tag, according to the manual of the 4-plex iTRAQ labeling kit (AB SCIEX, Framingham, MA, USA). The re-

constituted samples (50 μ L) were used for NanoLC-MS/MS analysis (AB SCIEX).

2.10. Metabolome analysis

The liver samples were subjected to capillary electrophoresis-time of flight-mass spectrometry (CE-TOFMS) and capillary electrophoresis-triple quadrupole mass spectrometry (CE-QqQMS) analyses, and the plasma samples were subjected to CE-TOFMS analysis (Agilent, Palo Alto, CA, USA) as described by Soga et al. (Soga et al., 2002, 2003). We performed a principal component analysis (PCA) with SampleStat ver. 3.14. Normalized metabolomics data were hierarchically clustered on both the metabolite and sample axes for a heat map representation and further analyzed by PCA using MeV software (Human Metabolome Technologies).

2.11. Statistical analysis

The results are presented as mean value \pm standard error (SE). Data were analyzed using one-way analysis of variance (ANOVA), and significant differences of means were evaluated with Dunnett's test at the level of $*p < 0.05$; $**p < 0.01$ vs. DSS group or $*p < 0.05$; $**p < 0.01$ vs. CON group. DAI was evaluated using non-parametric methods: the Kruskal-Wallis and Steel's test at the same level.

3. Results

3.1. General characteristics

No significant differences among the three groups were observed in total food intake (CON: 60.3 ± 1.0 ; DSS: 60.2 ± 5.1 ; DSSPAR: 60.3 ± 2.6 g), water intake (CON: 26.5 ± 0.6 mL), or DSS intake (DSS: 24.2 ± 1.5 ; DSSPAR: 25.1 ± 1.3 mL). DSS administration was associated with significant clinical changes, including weight loss (Fig. 1A) and the appearance of occult fecal blood and diarrhea, resulting in a significant increase in DAI compared to the CON group (Fig. 1B). PAR supplementation suppressed these pathological conditions of IBD, resulting in significant amelioration of DAI on day 8 and day 9 (Fig. 1B). The DSS mice had significantly shorter colon lengths (Fig. 1C) and lower relative mesenteric fat weight (Fig. 1D) compared to the CON mice, and PAR significantly ameliorated these decreases.

3.2. Biochemical analysis

The IL6 plasma levels were significantly increased by DSS administration, and PAR supplementation attenuated this increase (Fig. 1E). Plasma levels of SAA1 was also significantly ($p = 0.01$) lower in DSSPAR (33.5 ± 3.8 ng/mL) than DSS (47.5 ± 6.8 ng/mL) group. Significantly elevated plasma MMP3 concentrations were observed in DSS group (4.6 ± 0.2 ng/mL) as compared to CON (3.6 ± 0.2 ng/mL) group, however, PAR intervention strongly tended to lower this increase (4.0 ± 0.3 ng/mL; $p = 0.06$).

3.3. Colon histology

DSS induced a significant loss of crypts and the infiltration of inflammatory cells into the mucosa and submucosa

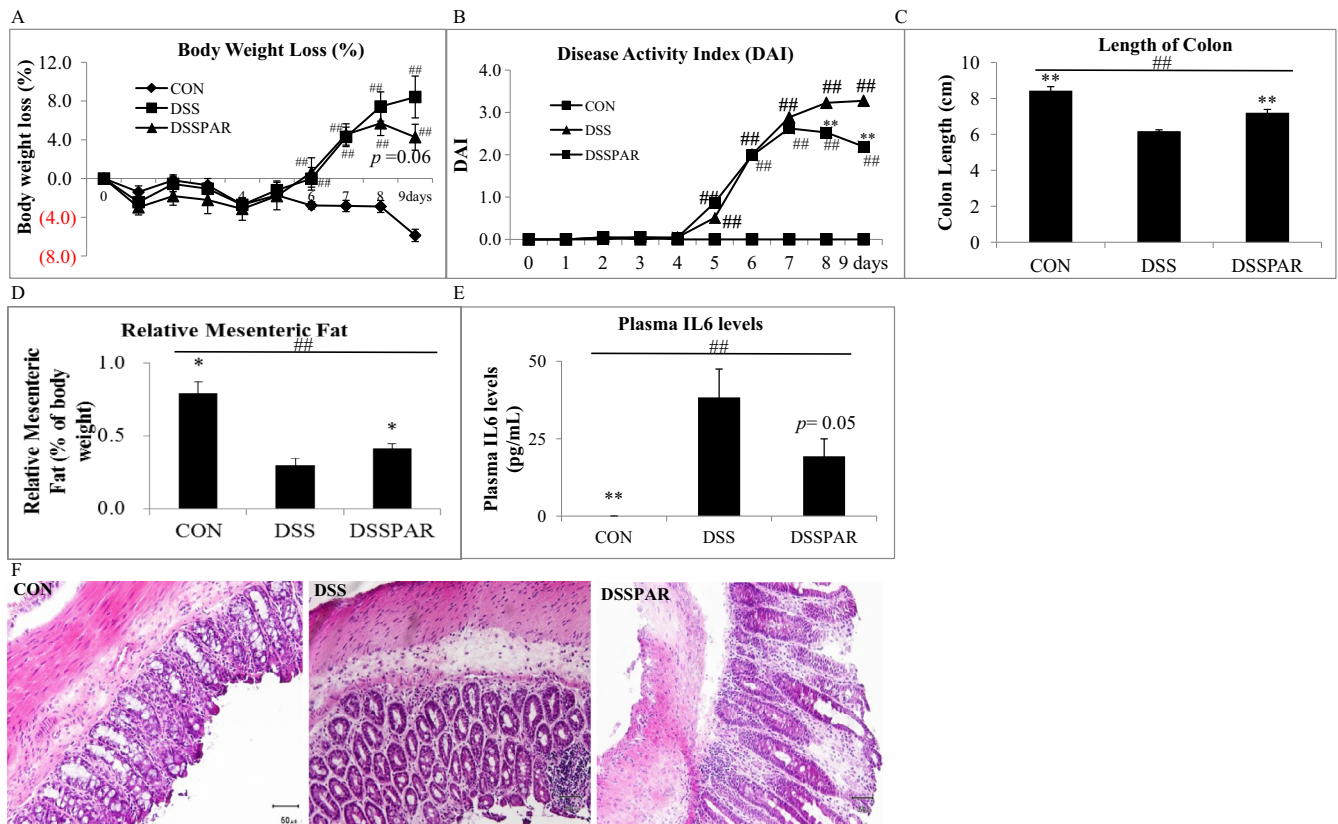


Fig. 1 – General characteristics of the study groups. (A) Body weight loss; (B) disease activity index (DAI); (C) length of colon; (D) relative mesenteric fat weight; (E) plasma IL6 levels; (F) H&E staining of colon. All values expressed as mean \pm SE ($n = 7$) ($*p < 0.05$; $p < 0.01$ vs. DSS group; $\#p < 0.05$; $\#\#p < 0.01$ vs. CON group by Dunnett's test).**

compared to the CON group. In the DSSPAR group, PAR supplementation mitigated the loss of crypts and tended to reduce the infiltration of inflammatory cells into the colonic mucosal wall (Fig. 1F).

3.4. Colonic microarray analysis

Among the total analyzed genes to identify colonic gene expressions associated with DSS administration and PAR supplementation, 2189 genes were differentially expressed in the DSS mice compared to the CON group. In the DSSPAR groups, 125 genes were up-regulated and 235 genes were down-regulated compared to the DSS group. The list of differentially changed genes is further detailed in [Supplementary Table S2](#).

PAR down-regulated the gene expression levels of the following members of the matrix metalloproteinase (MMP) family, which are involved in the breakdown of the extracellular matrix and tissue remodeling in normal physiological processes and disease progression: *Mmp3*, *Mmp10*, *Mmp13*, *Mmp19* and tissue inhibitor of metalloproteinase 1 (*Timp1*). The expression levels of the following chemokines, members of the chemokine (C-X-C motif) ligand (Cxcl) family, were also decreased: *Cxcl1*, *Cxcl3*, *Cxcl5*, *Cxcl6*, *Cxcl9* and *Cxcl12* and chemokine (C-C motif) ligand (Ccl): *Ccl11* and *Ccl5*.

In addition, decreases in the expression levels of the following proinflammatory cytokines: secreted phosphoprotein 1 (*Spp1*), and members of the IL family were observed: *IL1r1*,

IL6 and *IL6st*. Other down-regulated genes included haptoglobin (*Hp*), which plays a vital role in the susceptibility to IBD and DSS-induced murine colitis ([Marquez et al., 2011](#)); prostaglandin-endoperoxide synthase 2 (*Ptgs2*), a key factor in inflammatory cellular response; and cluster of differentiation163 (*Cd163*) which is commonly expressed in IBD patients ([Franzè et al., 2013](#)). From the results of the validation by real-time RT-PCR (Fig. 2), DSS significantly up-regulated the expression of *Mmp10*, *Timp1*, *Cxcl1*, *Cxcl9*, *Hp* and *Il6* and tended to increase the expression of *Mmp13*, *Mmp3*, *Ccl5*, *Cxcl6*, *Spp1* and *Cd163*. PAR supplementation significantly attenuated the increases in *Mmp3*, *Mmp10*, *Hp*, *Il6*, *Timp1*, *Ccl5* and *Cd163* and tended to suppress the up-regulation of *Cxcl1*, *Cxcl6*, *Cxcl9*, *Mmp13*, *Spp1* and *Ptgs2*.

3.5. Hepatic microarray analysis

Among the total analyzed genes in liver, 2219 were differentially expressed in the DSS group compared to the CON mice. In the DSSPAR group, 294 genes were up-regulated and 292 genes were down-regulated compared to the DSS mice. We have appended the list of differentially changed genes in [Supplementary Table S3](#).

PAR supplementation decreased the gene expression molecules involved in macrophage and lymphocyte signaling: vascular cell adhesion protein 1 (*Vcam1*), and that of the cancer markers serum amyloid A1 (*Saa1*), c-Jun (*Jun*) and S100 calcium

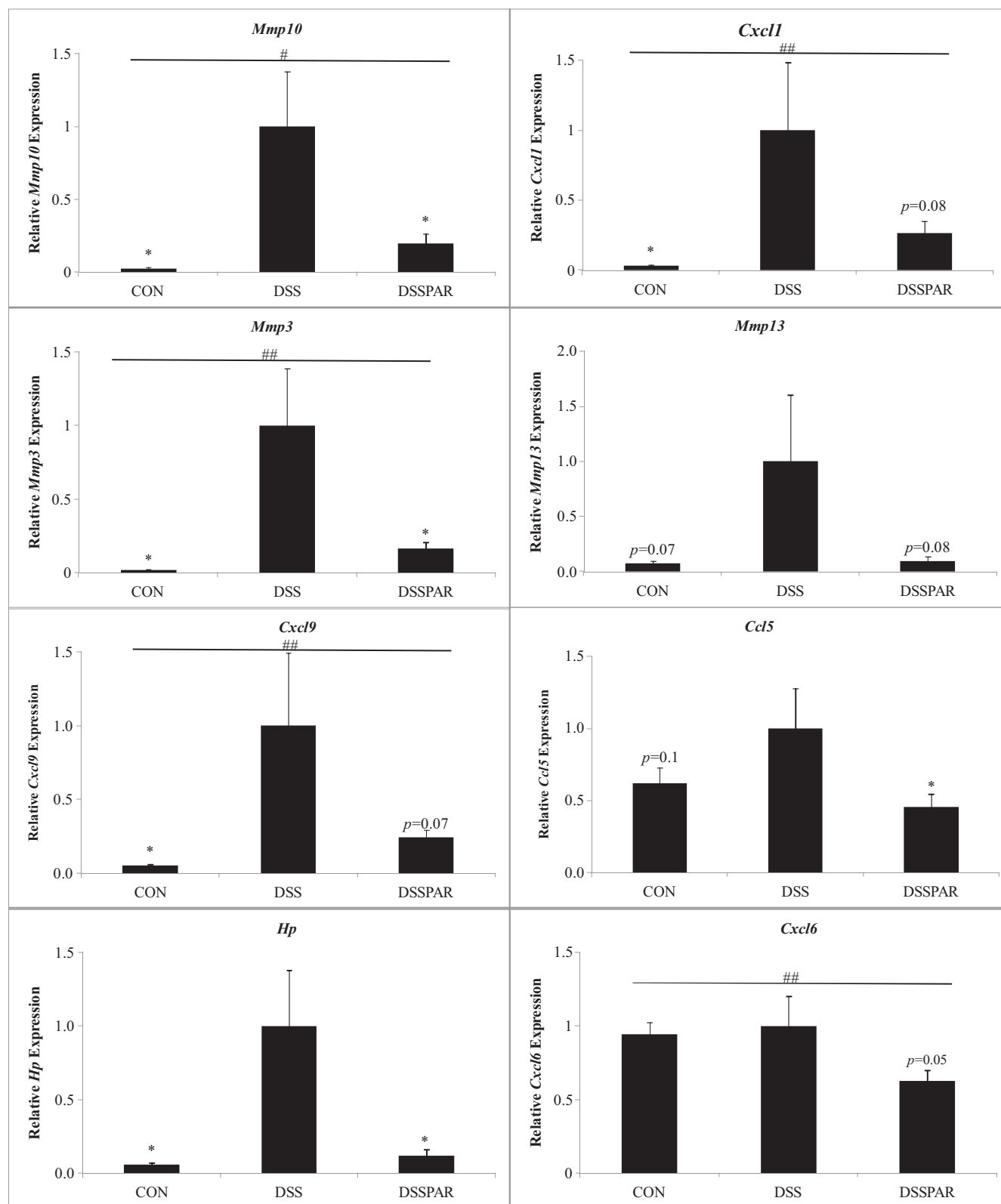


Fig. 2 – Colonic mRNA expressions of genes related to breakdown of the extracellular matrix and tissue remodeling, inflammation and IBD. The relative mRNA expressions of *Mmp3*, *Mmp10*, *Mmp13*, *Timp1*, *Ccl5*, *Cxcl1*, *Cxcl6*, *Cxcl9*, *Spp1*, *Hp*, *Il6*, *Ptgs2*, *Il6st* and *Cd163* were measured by RT-PCR and normalized to *Rplp1*. All values expressed as mean \pm SE ($n = 7$) (* $p < 0.05$; ** $p < 0.01$ vs. DSS group; # $p < 0.05$; ## $p < 0.01$ vs. CON group by Dunnett's test).

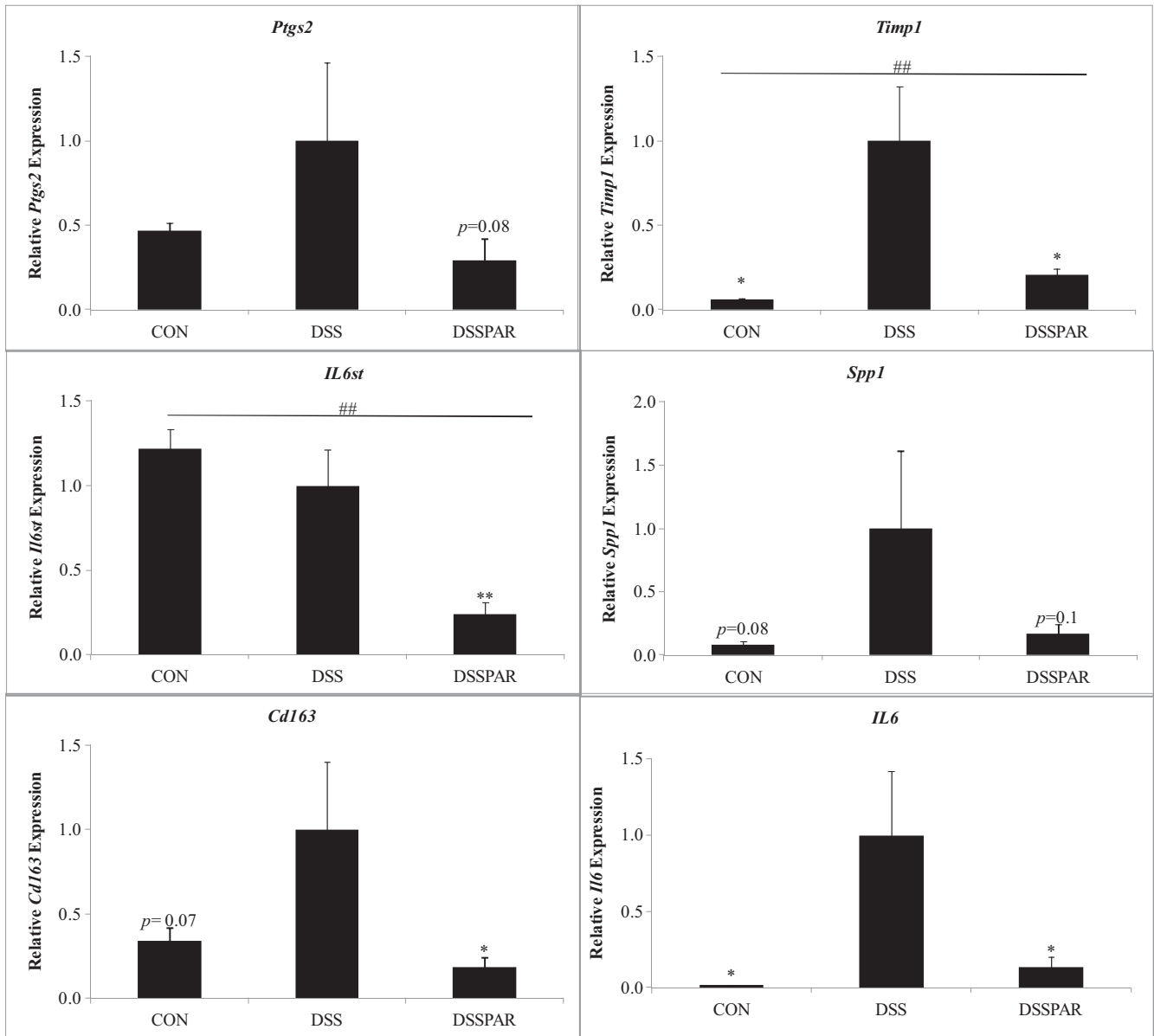


Fig. 2 – (continued)

binding protein A8 (S100A8). Genes involved in the urea cycle, i.e., argininosuccinate lyase (*Oat*) and arginase (*Arg1*), were down-regulated. In addition, the following genes involved in the citric acid cycle were up-regulated: phospholipase A2 (*Pla2g*), stearoyl-CoA desaturase-1 (*Scd1*), ELOVL family member 6, elongation of long chain fatty acids (*Elovl6*), fatty acid synthase (*Fas*), malate dehydrogenase 1 (*Mdh1*) and NADP-dependent malic enzyme (*Me1*). The gene expression level of methionine adenosyltransferase II, alpha (*Mat2a*), which is involved in the methionine recycling pathway was increased, and that of glutamic-oxaloacetic transaminase 1 (*Got1*), which is involved in the oxaloacetate–aspartate shuttle was decreased. According to the results of real-time RT-PCR, we found that DSS significantly regulated the expressions and PAR supplementation significantly mediated the expression of *Arg1*, *Elovl6*, *Fas*, *Got1*, *Jun*, *Mat2a*, *Me1*, *Scd1* and *S1008* (Fig. 3).

3.6. Comparative proteomics analysis by iTRAQ

We included a 1.2- or 0.8-fold cut-off from 895 unique proteins quantified at more than a 95% confidence level when classifying proteins as significantly up- or down-regulated. According to this criterion, we screened 222 proteins, of which 99 proteins were down-regulated and 123 proteins were up-regulated in DSSPAR compared to the DSS group (Supplementary Table S4).

PAR supplementation down-regulated the expression levels of the following: cancer-related proteins: protein S100-A11, Bcl-2-like protein 1, myeloid-associated differentiation marker, serum amyloid A-2 protein, cell death regulator *aven*, cullin-4B, periplakin, serum amyloid A-1 protein and serum amyloid P-component; diarrhea-related proteins: aquaporin 9; fibronective proteins: collagen alpha-1(I) chain and collagen

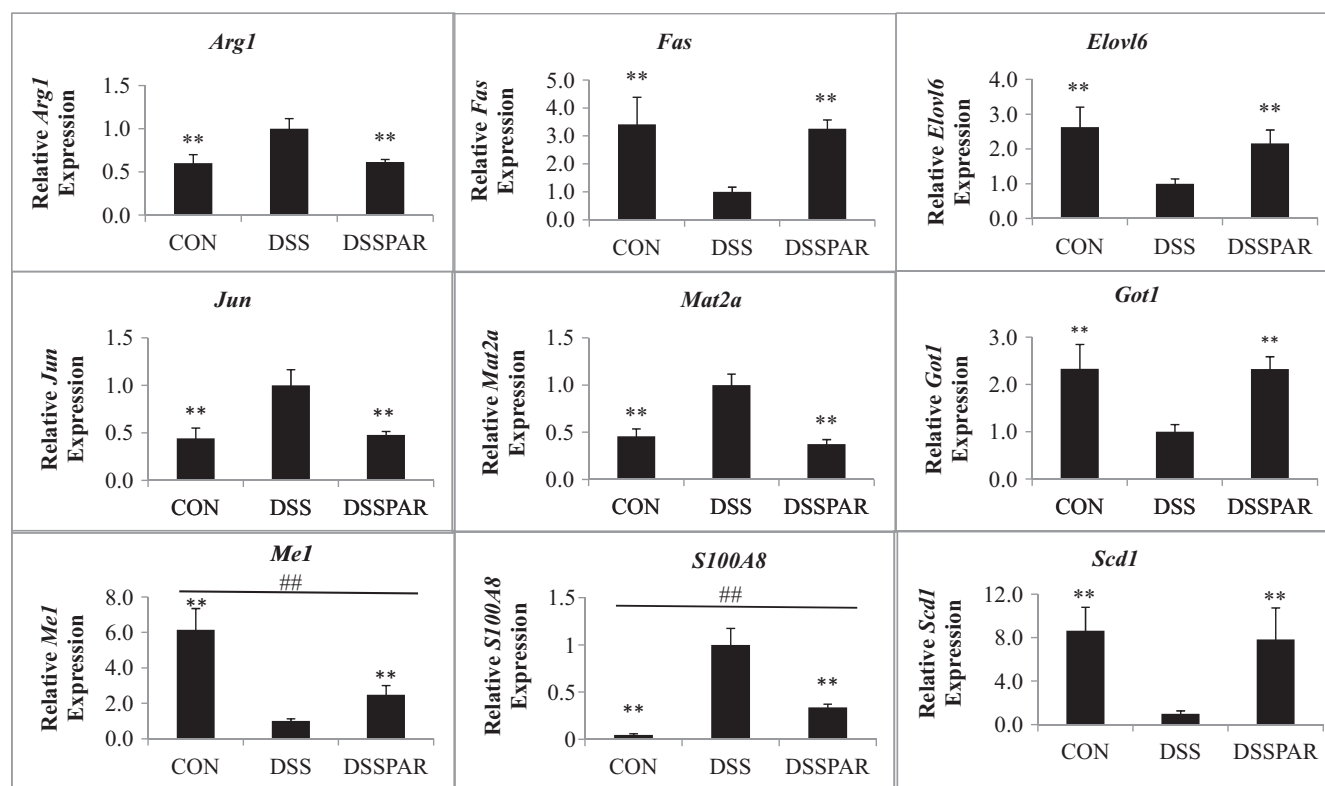


Fig. 3 – Hepatic mRNA expressions of genes related to cancer markers, genes involved in the citric cycle, urea cycle and methionine recycling pathway and fatty acid synthesis genes. The relative mRNA expressions of *Arg1*, *Elovl6*, *Fas*, *Got1*, *Jun*, *Mat2*, *Me1*, *Scd1* and *S100A8* were measured by RT-PCR and normalized to *Rplp1*. All values expressed as mean \pm SE ($n = 7$) (* $p < 0.05$; ** $p < 0.01$ vs. DSS group; # $p < 0.05$; ## $p < 0.01$ vs. CON group by Dunnett's test).

alpha-2(VI) chain; proteins involved in fatty acid oxidation: sphingomyelin phosphodiesterase 3, sphingosine-1-phosphate phosphatase 1, malectin, serine/threonine-protein phosphatase 4 regulatory subunit 3A; gamma-butyrobetaine dioxygenase; urea cycle proteins: asparaginyl-tRNA synthetase cytoplasmic; and proteins involved in glycolysis: alpha-amylase 1, succinate dehydrogenase assembly factor 1, and cystathionine gamma-lyase, a key protein in the methionine-recycling pathway.

The up-regulated proteins in the DSSPAR group include proteins that are involved in the citric cycle: NADP-dependent malic enzyme, NADH dehydrogenase [ubiquinone] flavoprotein 3, mitochondrial, glutathione S-transferase P1; proteins involved in the urea cycle: ornithine aminotransferase, mitochondrial, glutathione S-transferase P1, glutamine synthetase, and methionine-R-sulfoxide reductase B1, an enzyme of the methionine-recycling pathway.

3.7. Plasma and hepatic metabolome evaluation

We analyzed the metabolic profiles of liver and plasma in mice of the CON, DSS and DSSPAR groups where 116 and 127 metabolites were measured, respectively.

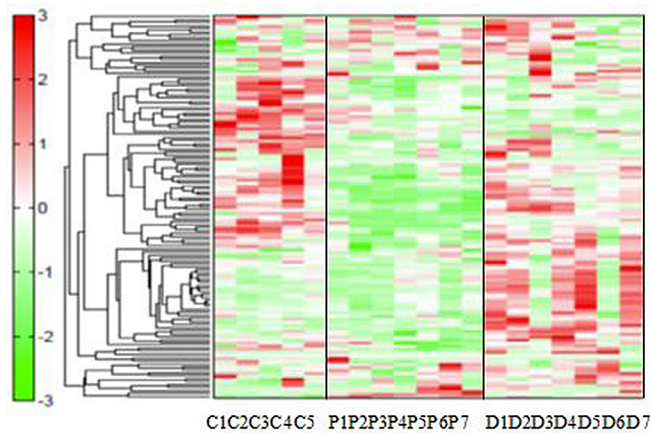
Distinct differences among the groups were observed in the heatmap and PCA of both plasma and liver metabolites (Fig. 4A, B). Twenty-five metabolites in plasma and 24 metabolites in liver were significantly regulated by DSS administration and sub-

sequently improved by PAR supplementation (Supplementary Table S5 for plasma and Supplementary Table S6 for liver). These metabolites include essential and non-essential amino acids (AA): asparagine (Asn), aspartic acid (Asp), alanine (Ala), serine (Ser), threonine (Thr), methionine (Met), valine (Val), and isoleucine (Ile); and elements of the urea cycle: urea, ornithine, arginine and intermediates of the methionine-recycling pathway including cystathionine. The data of the hepatic total glut-related AA, total AA, total pyr-related AA, total glucogenic AA, total non-essential AA and the NADH/NAD⁺ ratio also indicated that the PAR supplementation improved enhanced glycolysis and lactate fermentation, which is common in inflamed environments.

4. Discussion

Inflammatory responses in the colon begin with an infiltration of neutrophils and macrophages (Xavier & Podolsky, 2007), and that activated macrophages produce a potent mixture of broadly active inflammatory cytokines, including *IL6*, *IL1* and tumor necrosis factor-alpha (TNF- α) (Podolsky, 2002). In DSSPAR group, the heightened inflammatory spurt and secretion of metalloproteinases were muted by PAR supplementation, as the global colon gene expression and RT-PCR validation revealed a significant down-regulation of *IL6* and its downstream *Cd163* antigen, *Mmp10* and *Hp*. The expression of *IL6st*, the

A Heatmap and PCA of plasma metabolome



B Heatmap and PCA of liver metabolome

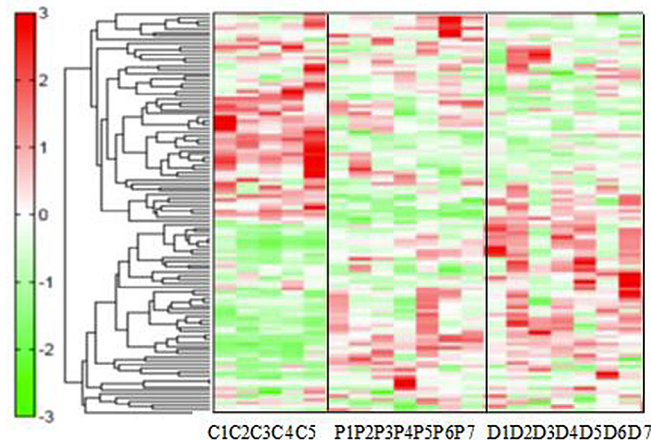


Fig. 4 – Normalized metabolomics data were hierarchically clustered on both the metabolite and sample axes for a heatmap representation and further analyzed by PCA using MeV software. Distinct differences among the groups were observed in the heatmap and PCA analysis of both (A) plasma and (B) liver metabolites.

regulator of *Hp* and *IL6*, and *Ccl5*, CCAAT/enhancer binding protein (*C/EBP*), delta (*Cebpd*) and *Mmp3*, the regulators of *Mmp10*, were also significantly reduced with PAR supplementation.

The expression of *Hp*, which is commonly upregulated in IBD patients (Marquez et al., 2011), has been described as a marker of inflammation due to its antioxidative properties. The transcriptional activation of the *Hp* by *IL6* results in the activation of *C/EBP* (Ramji, Vitelli, Tronche, Cortese, & Ciliberto, 1993), which was similarly observed in our study (DSS: 0.8 ± 0.3 ; DSSPAR: 0.2 ± 0.1 ; DSSPAR vs. DSS $p < 0.05$). Coupled with lowered *IL6* gene expression, plasma *IL6* levels were also significantly lowered by the PAR supplementation, indicating lowered systemic inflammation. Matrix metalloproteinases, in particular *Mmp3*, are capable of degrading a broad range of extracellular components (Stetler-Stevenson, 1990), which may lead to the degradation of the mucosal wall in IBD patients (Bailey et al., 1994). In addition to a significant decrease in *Mmp3* gene expression levels, lower plasma MMP3 concentrations in PAR couple the results of colon transcriptome showing that type IX, type X and type XI collagens, laminin and fibronectin were all differentially up-regulated in the DSS group and down-

regulated in the DSSPAR group. The mitigation of the degradation of colon mucosal crypt walls observed in the PAR-supplemented mice may be due, in part, to the down-regulation of metalloproteinases. In addition, *Timp1* was significantly down-regulated, and this was also observed in its downstream target, *IL1r1*. The expression levels of *Mmp13* where its upstream regulator is *Timp1*, and *Cxcl9*, the downstream molecule of *IL1r1*, tended to be reduced by PAR intervention. These results indicate that PAR supplementation significantly ameliorated the inflammation in the colon, which may prevent the degradation of the mucosal wall.

Direct downstream targets of released endotoxins and bacterial infection, the reason of accelerated DSS-induced colitis (Chen et al., 2008), including proinflammatory cytokines such as *ILs* and *TNF α* , can also suppress the expression of *SCD1* in the liver which has been identified and characterized as an early event prior to IBD clinical symptoms (Chen et al., 2008). Since in the present study the expression levels of *IL6*, *Cxcl1*, *Cxcl6*, *Cxcl9*, and *Ccl5* were dramatically increased by DSS treatment, it is likely that a portal vein delivery of inflammatory markers from the colon may contribute to the suppression of

Scd1 expression in liver. PAR supplementation down-regulated colonic cytokine expression, leading to a decrease in cytokines delivered to the liver thereby resulting in the up-regulation of *Scd1*, in that reducing the severity of colitis. This may also related with significantly lower plasma and hepatic levels of cancer marker-Saa1 in DSSPAR mice.

During inflammation, a large number of immune cells are recruited to inflammatory lesions. Cell migration, phagocytosis, bacteria killing and stimulated cell proliferation have high energy demands (Borregaard & Herlin, 1982). Neutrophils, macrophages, and dendritic cells primarily use glycolytic pathways to obtain energy, whereas B and T cells use mainly amino acids, glucose and lipids to generate energy during oxidative phosphorylation. The metabolome analysis revealed that compared to DSS group, PAR induced significant decreases in plasma amino acids related to pyruvate (Ala, Ser and Thr), oxaloacetate (Asn and Asp), and succinyl coA (Met, Val and Isoleucine), which are elements of the citric cycle. Total glucogenic amino acids were also significantly reduced by PAR dietary intervention. These indicate impaired glycolysis and oxidative phosphorylation manifested by reduced inflammation in the DSSPAR group. In addition, as an inflammatory marker of neutrophil activation, PAR dietary intervention tended ($p = 0.09$) to improve elevated MPO levels induced by DSS administration (CON: 5.9 ± 2.3 mU/mL; DSS: 13.3 ± 4.0 mU/mL; PAR 6.9 ± 2.0 mU/mL). Our evaluation of the hepatic transcriptome coupled with RT-PCR validation also indicated that PAR supplementation induced a significant up-regulation of genes involved in the intermediates of citric cycle—*Fas*, *Me1*, *Scd1* and *Elovl6*. The metabolic shifts in the citric cycle as well as the up-regulation of fatty acid synthesis related genes could be reflected in the improved body weight loss and relative mesenteric fat in the DSSPAR mice.

IBD patients often present with a negative nitrogen balance, and arginine (Arg), which is a semi-essential amino acid that is important in protein synthesis, plays a key role in the intermediate metabolism of nitrogen by participating in the urea cycle. Arg is also a substrate for nitric oxide (Coman, Yapliito-Lee, & Boneh, 2008) and a precursor to glutamine, proline, and ornithine (Wu & Morris, 1998). The expression level of *Arg1*, which is involved in the conversion of arginine to urea and arginine to ornithine, was significantly decreased in the liver of DSSPAR mice, which may explain the lower levels of urea in the liver, and of arginine and ornithine in their plasma. As such, the ameliorative properties of PAR in colitis may be in part due to an improved nitrogen balance in the liver, contributing to reduced oxidative stress.

Inflammatory responses in the colon are accompanied by striking shifts in tissue metabolism with respect to cellular methylation reactions (Kominsky et al., 2011). In DSSPAR group, we observed a significant down-regulation of *Mat2a*, the gene that encodes for *Mat2a*—the enzyme responsible for the production of S-adenosylmethionine, which is the methyl donor for the majority of methylation reactions. A metabolite downstream of S-adenosylhomocysteine, cystathionine, as well as a related enzyme, cystathionine gamma-lyase from proteome were significantly down-regulated, indicating a shift to methylation inhibition may have occurred in the PAR-supplemented mice. Cystathionine is converted into cysteine by cystathionine gamma-lyase. The indirect increased biosynthesis of

cysteine (a precursor of glutathione) is an indication of the oxidative stress state in the inflamed gastrointestinal tract (Miller et al., 2013). In addition, riboflavin metabolism, which is required to convert glutathione between its oxidized and reduced forms, is increased during inflammation. Both riboflavin and NADPH, a product of the pentose phosphate pathway, are necessary for regenerating oxidized glutathione back to its reduced form, and are thus essential for pH and oxidative stress homeostasis (Massey, 2000). The recovery of oxidative stress in DSSPAR mice was complemented by the significant improvement in NADH/NAD⁺ by PAR supplementation (Massudi, Grant, Guillemin, & Braid, 2012). This effect could be due in part to the high concentrations of riboflavin in PAR (Supplementary Table S7) which may compensate for increased riboflavin metabolism during inflammation.

5. Conclusions

Through our nutriomics study, we have accumulated robust scientific knowledge of nutrient signals and the imprint of PAR on systems biology. The nutrition-relevant colon transcriptome revealed a decrease in the expression of inflammatory cytokines and fibrotic markers, resulting in reduced inflammation and improved colon shortening. The dietary signature of PAR on the hepatic transcriptome and proteome, which is complementary to that of the metabolome, showed a decrease in the expression of carcinogenic markers, thereby reducing cancer risk; increases in the expression of fatty acid synthesis-related markers, thereby improving body weight loss; an up-regulation of molecules involved in the citric acid cycle and urea cycle suggesting recovery in both glycolysis and oxidative stress. Markers in the methionine-recycling pathway were down-regulated resulting in a shift to methylation inhibition and reduced inflammation. The clues from each analysis complement each other, completing the PAR-colitis puzzle, successfully leading to the crucial findings of the present study (Fig. 5).

Our study is a pioneering effort to obtain a precise understanding of PAR as a novel and effective nutraceutical in optimal IBD management using multifaceted integrated omics analyses. Our unique synergistic approach is of significant importance since no single omics approach can fully illustrate the intricate beauty behind the relatively modest influence of food factors. We sincerely anticipate that the methods of this study will serve as a clarion call to promote integrated omics nutrition research to uncover new dietary intervention strategies designed to recover normal homeostasis in disease states and to maintain healthy well-being, bringing forward a new evolution in nutritional science.

Acknowledgements

This study was supported in part by a grant-in-aid for JSPS Postdoctoral Fellowship for Foreign Researchers Fellows from the Japan Society for the Promotion of Science. We would like to thank Professor Masatoshi Hori, Graduate School of Agricultural and Life Sciences, The University of Tokyo, who gave us

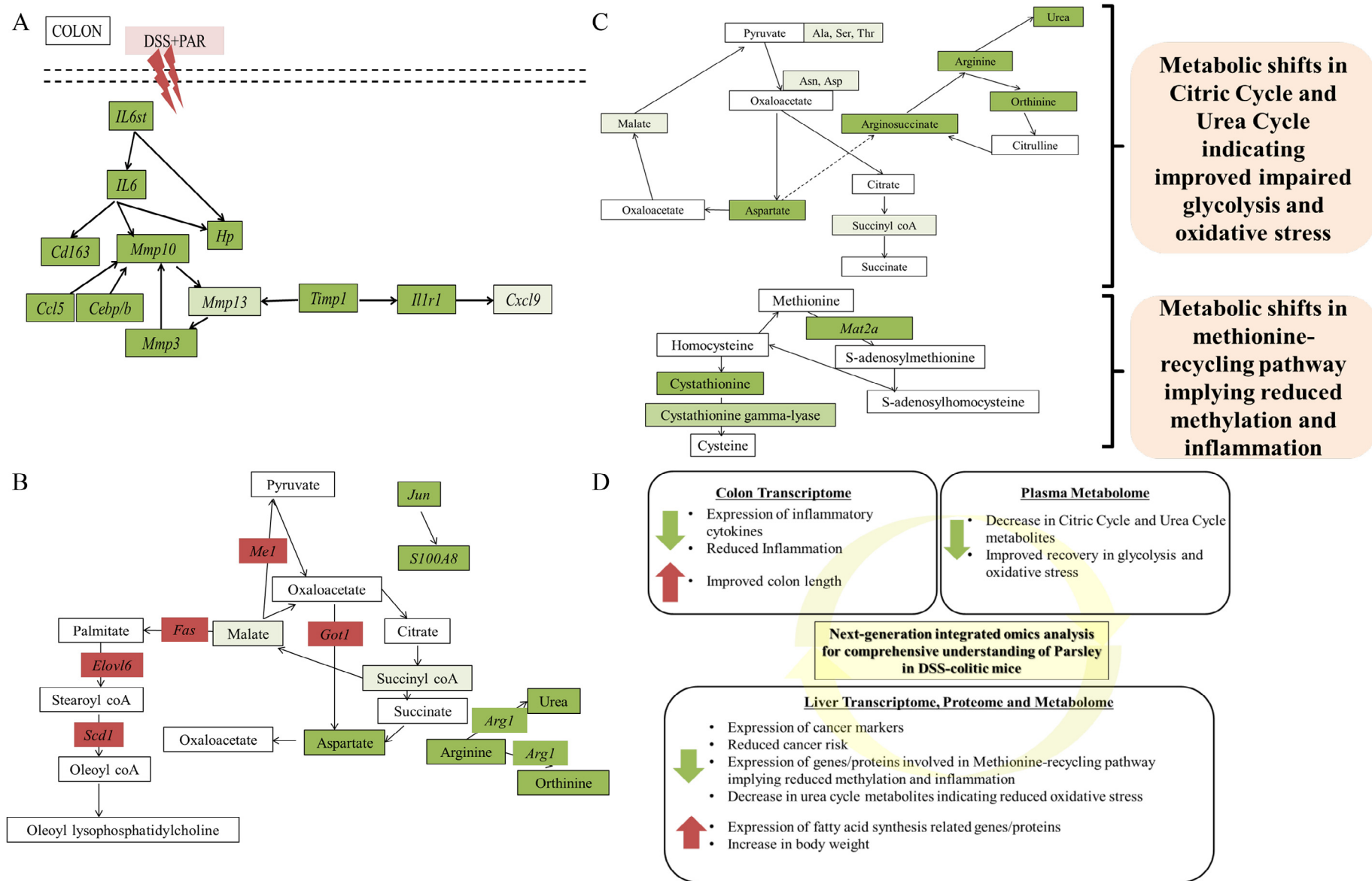


Fig. 5 – Schematic representation of the integrated comprehensive analysis of PAR's effects on the DSS-colitic mouse model. (A) Nutrition-relevant colon transcriptome; (B) dietary signature of PAR on the hepatic transcriptome and proteome; (C) the influence of PAR supplementation on plasma metabolome, hepatic proteome and metabolome; (D) evidence-based insight into the influence of PAR supplementation on colitis. The genes in light green ovals had a strong tendency for improvement, whereas the genes in dark green or dark red ovals indicate that a significant improvement followed the PAR supplementation. (For interpretation of the references to color in this figure legend, the reader is referred to the web version of this article.)

valuable advice. We also sincerely thank Human Metabolome Technologies for supporting the part of metabolome analysis. H.J. and W.A. designed the research; H.J., W.A. and M.H. conducted the experiments; H.J., W.A., S.T., and H.T. analyzed the data; K.S. and M.T. performed the statistical analysis; and H.J. and W.A. wrote the paper. H. K. had primary responsibility for the final content. All authors read and approved the final manuscript.

Appendix: Supplementary material

Supplementary data to this article can be found online at doi:10.1016/j.jff.2014.09.018.

REFERENCES

- Bailey, C., Hembry, R., Alexander, A., Irving, M., Grant, M., & Shuttleworth, C. (1994). Distribution of the matrix metalloproteinases stromelysin, gelatinases A and B, and collagenase in Crohn's disease and normal intestine. *Journal of Clinical Pathology*, 47, 113–116.
- Baumgart, D. C., & Carding, S. R. (2007). Inflammatory bowel disease: Cause and immunobiology. *The Lancet*, 369, 1627–1640.
- Borregaard, N., & Herlin, T. (1982). Energy metabolism of human neutrophils during phagocytosis. *The Journal of Clinical Investigation*, 70, 550–557.
- Chen, C., Shah, Y. M., Morimura, K., Krausz, K. W., Miyazaki, M., Richardson, T. A., Morgan, E. T., Ntambi, J. M., Idle, J. R., & Gonzalez, F. J. (2008). Metabolomics reveals that hepatic stearoyl-CoA desaturase 1 downregulation exacerbates inflammation and acute colitis. *Cell Metabolism*, 7, 135–147.
- Coman, D., Yapliito-Lee, J., & Boneh, A. (2008). New indications and controversies in arginine therapy. *Clinical Nutrition (Edinburgh, Scotland)*, 27, 489–496.
- Franzè, E., Caruso, R., Stolfi, C., Sarra, M., Cupi, M. L., Caprioli, F., Monteleone, I., Zorzi, F., De Nitto, D., Colantoni, A., Biancone, L., Pallone, F., & Monteleone, G. (2013). Lesional accumulation of CD163-expressing cells in the gut of patients with inflammatory bowel disease. *PLoS ONE*, 26, e69839.
- Islam, M. S., Murata, T., Fujisawa, M., Nagasaka, R., Ushio, H., Bari, A. M., Hori, M., & Ozaki, H. (2009). Anti-inflammatory effects of phytosteryl ferulates in colitis induced by dextran sulphate sodium in mice. *British Journal of Pharmacology*, 154, 812–824.
- Jia, H., Saito, K., Aw, W., Takahashi, S., Hanate, M., Hasebe, Y., & Kato, H. (2013). Transcriptional profiling in rats and an ex vivo analysis implicate novel beneficial function of egg shell membrane in liver fibrosis. *Journal of Functional Foods*, 5, 1611–1619.
- Jia, H., Takahashi, S., Saito, K., & Kato, H. (2013). DNA microarray analysis identified molecular pathways mediating the effects of supplementation of branched-chain amino acids on CCl₄-induced cirrhosis in rats. *Molecular Nutrition and Food Research*, 57, 291–306.
- Justesen, U., Knuthsen, P., & Leth, T. (1998). Quantitative analysis of flavonols, flavones, and flavanones in fruits, vegetables and beverages by HPLC with photodiode array and mass spectrometric detection. *Journal of Chromatography. A*, 799, 101–110.
- Khor, B., Gardet, A., & Xavier, R. J. (2011). Genetics and pathogenesis of inflammatory bowel disease. *Nature*, 474, 307–317.
- Kominsky, D. J., Keely, S., MacManus, C. F., Glover, L. E., Scully, M., Collins, C. B., Bowers, B. E., Campbell, E. L., & Colgan, S. P. (2011). An endogenously anti-inflammatory role for methylation in mucosal inflammation identified through metabolite profiling. *The Journal of Immunology*, 186, 6505–6514.
- Marquez, L., Shen, C., Machiels, K., Perrier, C., Ballet, V., Organe, S., Ferrante, M., Henckaerts, L., Rutgeerts, P., Vermeire, S., Ceuppens, J., & Cleynen, I. (2011). Role of haptoglobin in susceptibility of IBD and in triggering murine colitis. *Gastroenterology*, 140, S–28.
- Massey, V. (2000). The chemical and biological versatility of riboflavin. *Biochemical Society Transactions*, 28, 283–296.
- Massudi, H., Grant, R., Guillemin, G. J., & Braid, N. (2012). NAD⁺ metabolism and oxidative stress: The golden nucleotide on a crown of thorns. *Redox Report*, 17, 28–46.
- McHenga, S. S. S., Wang, D., Li, C., Shan, F., & Lu, C. (2008). Inhibitory effect of recombinant IL-25 on the development of dextran sulfate sodium-induced experimental colitis in mice. *Cellular and Molecular Immunology*, 5, 425–431.
- Miller, J. W., Beresford, S. A., Neuhauser, M. L., Cheng, T. Y. D., Song, X., Brown, E. C., Zheng, Y., Rodriguez, B., Green, R., & Ulrich, C. M. (2013). Homocysteine, cysteine, and risk of incident colorectal cancer in the Women's Health Initiative observational cohort. *American Journal of Clinical Nutrition*, 97, 827–834.
- Podolsky, D. (2002). Inflammatory bowel disease. *The New England Journal of Medicine*, 347, 417–429.
- Ramji, D. P., Vitelli, A., Tronche, F., Cortese, R., & Ciliberto, G. (1993). The two C/EBP isoforms, IL-6DBP/NF-IL6 and C/EBP delta/NF-IL6 beta, are induced by IL-6 to promote acute phase gene transcription via different mechanisms. *Nucleic Acids Research*, 21, 289–294.
- Simon, J. E., & Quinn, J. (1988). Characterization of essential oil of parsley. *Journal of Agricultural and Food Chemistry*, 36, 467–472.
- Soga, T., Ohashi, Y., Ueno, Y., Naraoka, H., Tomita, M., & Nishioka, T. (2003). Quantitative metabolome analysis using capillary electrophoresis mass spectrometry. *Journal of Proteome Research*, 2, 488–494.
- Soga, T., Ueno, Y., Naraoka, H., Ohashi, Y., Tomita, M., & Nishioka, T. (2002). Simultaneous determination of anionic intermediates for *Bacillus subtilis* metabolic pathways by capillary electrophoresis electrospray ionization mass spectrometry. *Analytical Chemistry*, 74, 2233–2239.
- Stetler-Stevenson, W. (1990). Type IV collagenase in tumour invasion and metastasis. *Cancer Metastasis Reviews*, 9, 289–303.
- Wu, G., & Morris, S. J. (1998). Arginine metabolism nitric oxide and beyond. *The Biochemical Journal*, 336, 1–17.
- Xavier, R. J., & Podolsky, D. K. (2007). Unravelling the pathogenesis of inflammatory bowel disease. *Nature*, 448, 427–434.